AD_____

GRANT NUMBER DAMD17-94-J-4242

TITLE: Electrically Mediated Trauma Repair

PRINCIPAL INVESTIGATOR: Richard B. Borgens, Ph.D.

CONTRACTING ORGANIZATION: Purdue Research Foundation
West Lafayette, Indiana 47907

REPORT DATE: September 1996

TYPE OF REPORT: Annual

PREPARED FOR: Commander
U.S. Army Medical Research and Materiel Command
Fort Detrick, Frederick, Maryland 21702-5012

DISTRIBUTION STATEMENT: Approved for public release;
distribution unlimited

DISCLAIMER NOTICE

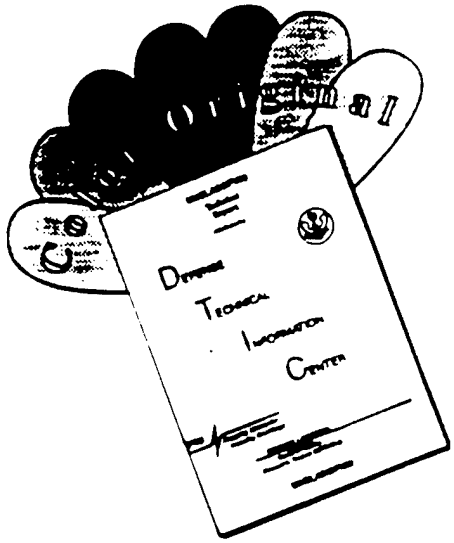

THIS DOCUMENT IS BEST QUALITY AVAILABLE. THE COPY FURNISHED TO DTIC CONTAINED A SIGNIFICANT NUMBER OF COLOR PAGES WHICH DO NOT REPRODUCE LEGIBLY ON BLACK AND WHITE MICROFICHE.

REPORT DOCUMENTATION PAGE

Form Approved
OMB No. 0704-0188

1. AGENCY USE ONLY *(Leave blank)*	2. REPORT DATE	3. REPORT TYPE AND DATES COVERED
	September 1996	Annual (22 Aug 95 - 21 Aug 96)

4. TITLE AND SUBTITLE
Electrically Mediated Trauma Repair

5. FUNDING NUMBERS
DAMD17-94-J-4242

6. AUTHOR(S)
Richard B. Borgens, Ph.D.

7. PERFORMING ORGANIZATION NAME(S) AND ADDRESS(ES)
Purdue Research Foundation
West Lafayette, Indiana 47907

8. PERFORMING ORGANIZATION REPORT NUMBER

9. SPONSORING/MONITORING AGENCY NAME(S) AND ADDRESS(ES)
Commander
U.S. Army Medical Research and Materiel Command
Fort Detrick, Frederick, MD 21702-5012

10. SPONSORING/MONITORING AGENCY REPORT NUMBER

11. SUPPLEMENTARY NOTES

12a. DISTRIBUTION / AVAILABILITY STATEMENT
Approved for public release; distribution unlimited

12b. DISTRIBUTION CODE

13. ABSTRACT *(Maximum 200*

In the second year of this contract period we have made substantial progress in experiments designed to facilitate recovery of functions following severe acute spinal cord injury in the adult mammal. The intervention is through the use of applied voltage gradients. We have shown that this technique can be used in conjunction with polymeric tubes to induce and guide regenerating axons. We have also developed novel two and three-dimensional reconstruction techniques and morphometry to assay our biological responses to treatment between control and experimental groups. Using these, we have assayed the level of macrophage infestation of acute and subacute spinal cord injuries. Furthermore, we have preliminary evidence of a direct effect of the applied voltage gradient on the accumulation of these cells during the early inflammatory response in addition to the responses of compromised nerve fibers. Since macrophages are now seen to produce both delayed and deleterious "bystander damage" to CNS parenchyma, reduction of their numbers at the injury zone may help explain the improved functional outcome demonstrated by this novel technique designed for early intervention following CNS injury.

14. SUBJECT TERMS	15. NUMBER OF PAGES
Neurotrauma, Spinal Cord, Paraplegia	19
	16. PRICE CODE

17. SECURITY CLASSIFICATION OF REPORT	18. SECURITY CLASSIFICATION OF THIS PAGE	19. SECURITY CLASSIFICATION OF ABSTRACT	20. LIMITATION OF ABSTRACT
Unclassified	Unclassified	Unclassified	Unlimited

FOREWORD

Opinions, interpretations, conclusions and recommendations are those of the author and are not necessarily endorsed by the US Army.

___ Where copyrighted material is quoted, permission has been obtained to use such material.

___ Where material from documents designated for limited distribution is quoted, permission has been obtained to use the material.

NA ___ Citations of commercial organizations and trade names in this report do not constitute an official Department of Army endorsement or approval of the products or services of these organizations.

NA ___ In conducting research using animals, the investigator(s) adhered to the "Guide for the Care and Use of Laboratory Animals," prepared by the Committee on Care and Use of Laboratory Animals of the Institute of Laboratory Resources, National Research Council (NIH Publication No. 86-23, Revised 1985).

___ For the protection of human subjects, the investigator(s) adhered to policies of applicable Federal Law 45 CFR 46.

___ In conducting research utilizing recombinant DNA technology, the investigator(s) adhered to current guidelines promulgated by the National Institutes of Health.

___ In the conduct of research utilizing recombinant DNA, the investigator(s) adhered to the NIH Guidelines for Research Involving Recombinant DNA Molecules.

___ In the conduct of research involving hazardous organisms, the investigator(s) adhered to the CDC-NIH Guide for Biosafety in Microbiological and Biomedical Laboratories.

PI - Signature Sept 3, 96 Date

Table of Contents

INTRODUCTION

This annual report covers the period 08/22/95 - 08/21/96 and provides details of continuing studies supported under USAMRMC contract # DAMD17-94-J-4242. Investigations concluded during the first year, and details of ongoing studies covered in the last annual report (November 21, 1995) will not be repeated here. A brief introductory note is included in each subsection to provide continuity between the last report and this present text.

BODY

I. NEW EXPERIMENTAL METHODS:

Quantitative Evaluation of Macrophage invasion of the subacute injury by Two and Three Dimensional Computer Morphometry

Large adult rats were used in this study. Approximately 40 animals were used to develop our techniques for computer assisted computation of macrophage numbers, 8 of these providing comprehensive data on the density of macrophage invasion of SCI at 3 weeks post injury, the level of cavitation of the tissue, and three dimensional volume and shape reconstruction of the injury zone. A total of 16 were used to study the effects of applied voltages (8 animals in the experimental group, 8 in the sham treated control group).

Animals

Fully adult (300 - 400 g) laboratory Rats (Sprague Dawley) were used in these experiments. Following surgery, they were housed two animals per cage, fed ad libidum, and their health monitored daily. Animals in this study were sacrificed 3 weeks (21 $\pm$ 1 days) post surgery by an overdose of Sodium Pentobarbital (0.8 ml of 1 g/ml Standard injectable) immediately followed by perfusion/fixation with 6% paraformaldehyde, 0.1% glutaraldehyde in a Phosphate buffer. The spinal cords were dissected free and immersion fixed in the above fixative for about 2 hours. The effects of applied voltages were evaluated approximately 2 months post injury.

Surgical procedures

Anesthesia was performed using an intraperioteneal injection of 1 ml/100g body weight of a standardized solution of 10 ml Ketamine HCL (100 mg/ml) and 1.1 ml Xylazine (100 mg/ml). The spinal cord was exposed by dorsal and partial laminectomy (dura intact), and a crush lesion was performed using blunted Watchmakers forceps. In an attempt to reduce variation in lesions, the

compression of the spinal cord was modeled after a method by Blight[1]. The incision was closed in layers with 3-0 proline suture, and the skin closed with wound clips which were sloughed about 2 weeks post surgery. Immediately post surgery each animal was subcutaneously injected with 3 ml lactated ringers to prevent dehydration, and the animal placed under a heat lamp for about 24 hours to reduce post surgical mortality due to shock.

Immunocytochemistry

The segment of spinal cord containing the lesion was dehydrated in ascending concentrations of alcohol followed by Xylene permitting infiltration and imbedding in Paraplast (paraffin) by conventional methods. Spinal cords were sectioned on a rotary microtome at approximately 15 microns, and sections affixed to microscope slides. Prior to use the slides were dipped in a 0.5% gelatin solution which aids in the adhesion of the sections to the slides during subsequent treatment. Paraffin was partially removed with a 1 hour treatment in a 60 °C oven, and completely removed after a 1 hour immersion in 100% Xylene. Sections were rehydrated by immersions in descending grades of alcohol to distilled water by conventional methods.

Hydrated sections affixed to slides were first incubated in a commercial enzyme and tissue non specific antigen blocker (Endoblocker M 69 and Tissue blocker, Biomedia) for 10, and 5 minutes respectively, with a 1 minute rinse in buffer (automation buffer, Biomedia). The sections are then exposed to the primary antibody for the macrophage; ED 1 (MCA - 341, Serotech/Harlan Bioproducts) for 10 minutes, and rinsed with buffer. The secondary antibody (rabbit - antimouse (Lab Probe, Biomedia) was administered for 10 minutes, rinsed in buffer prior to exposure to the horseradish peroxidase (10 minutes), rinsed, and exposed to a commercial prepared Diaminobenzidine reagent (Biomedia) for 5 minutes, and counter stained with Mayers Hematoxylin. Stained sections were rinsed in distilled water and coverslips affixed with a warm Glycerol Gelatin (Sigma).

Computer Assisted Morphometry

The method used for the most accurate counting of macrophage within histological sections was based on the determination of an average number of pixels represented by a single macrophage at a standardized magnification. By using software that can transform assigned color pixel values (CLUT's Color Look Up Tables) to a single color pixel value, the area of interest (assigned colors) can be measured in pixels. By sampling every third section at approx. 15 µm, more target area, comprised of labeled cells, can be evaluated within histological sections than is practical by other sampling/counting techniques. Furthermore, once the visual data is digitized, transformed for counting, and assigned a file name - the actual counting can be performed using a custom designed program that does not require human interaction with the acquisition of this data. We employ RastorOps Media Grabber© to capture 80-100% of the lesion at 20 X magnification using a JVC color video camera ported to an

Olympus VanOx Universal Microscope. Morphometry is accomplished using IP Lab Spectrum© software and custom designed software developed at Purdue (see below).

II. RESULTS AND DISCUSSION

Macrophage Size in Pixels

At a standardized magnification of 200 diameters, an average of 14 ± 5 individual macrophage cells (full diameter and isolated from other cells) were chosen per histological section from a series of 12 slides. The mean, SD, and SEM of these 173 cells in pixels was 18.87, 4.17, and 0.32 respectively. The actual unit area of the pixel at this same magnification in micrometers was determined by capturing an index score of a haemocytometer to the computer to derive the unit area in micrometers for each macrophage. We also made measurements of 61 similar macrophages, approximate full diameter and isolated from other cells using an eyepiece ocular micrometer for comparison of the means.

Verification: Macrophage Cell Diameter and Cell Counting

As described previously, the mean cell diameter in pixels of 173 individually measured cells was 18.9 + 0.3, while the mean diameter by actual measurement was 12.5 + 2.7 uV. We compared this average diameter with other histological examples of macrophages taken from the literature, and we made micrometer measurements of 61 individual and isolated macrophages as an additional check. In brief, our computer derived estimate of the macrophage cell diameter was clearly similar to those previously presented for both laboratory rats and guinea pigs. Computer derived cell diameters and direct measurement of macrophage diameters (using an ocular micrometer) were not significantly different (**Table 1**).

Table 1

Type of Measurement	Animal N	Number of macrophages measured	Mean cell diameter (pixels)	Mean cell diameter (μm)	SD (μm)	SEM (μm)	Mann-Whitney U (2-tailed, unpaired)
Visual	8	61	18.87*	12.47	2.76	0.21	P = 0.7201
Computer	12	173	N/A	12.77	3.89	0.50	

* 1 μm = 1.5135 pixels (20x objective Olympus Van Ox microscope)

The accuracy of our computer assisted computation of macrophage number based on pixel values was verified by comparing computer assisted counts of

macrophages within 10 different fields of view at our standard field of view(200 diameters magnification) with investigator counts of these same fields of view. These numbers were very close, and were not different statistically (**Table 2**).

Table 2

Type of Measurement	Animal N	Number of areas counted	Mean macrophage count	SD	SEM	Wilcoxon (2-tailed, paired)
Visual	7	10	55.60	50.75	16.05	P = 0.5566
Computer	7	10	59.50	67.27	21.27	

In every injured spinal cord, macrophages were the dominate cell type occupying the site of damage. Given the dorsal approach to the spinal cord during the hemilaminectomy procedure followed by compression of the dorsal funiculus, one would reasonably expect the lesion severity to be most profound in this region in all eight spinal cords. Figure 1 shows 3 sets of data from three individual rat spinal cords (Fig. 1A), while Figure 1B shows the average of all eight animals. The hatched bar in Figure 1B is the mean for macrophage number, the mean for macrophage area is the solid bar. (Means and error bars are approximately identical for both values).

The boundary of the injured region of spinal cord was conspicuous due to large accumulations of labeled macrophages separating intact parenchyma (well visualized by our counter stain) from phage infested and usually cavitated spinal cord parenchyma. This was especially true of all eight spinal cords in regions of gray matter, while the boundary between injured and uninjured parenchyma was more irregular in white matter. While the integrity of adjacent " intact " spinal cord tissue was apparently normal (showing well defined cell borders, homogeneous staining with hematoxylin, and free of phagocytes) these regions did possess variable amounts of cavitation. Though we made no comprehensive effort to quantitate the various fluid filled cavities that form in response to spinal cord contusion and compression, we did measure the diameters of two separate types of cavities that were common in all eight cords studied. Large cysts that were centrally located within the region of injury and appeared to be in continuity with the swollen central canal (syrinx) were on the order of 0. 3 mm (n=62) Thus the large cavities in central regions of gray matter were on the order of 1/8 th the diameter of the uninjured spinal cord. In all spinal cords but two, the segment of the central canal was more swollen rostral to the injury than caudal, however we detected no statistical difference in the size of the large cysts in these areas relative to the rostral/caudal side of the injury in which they occurred.

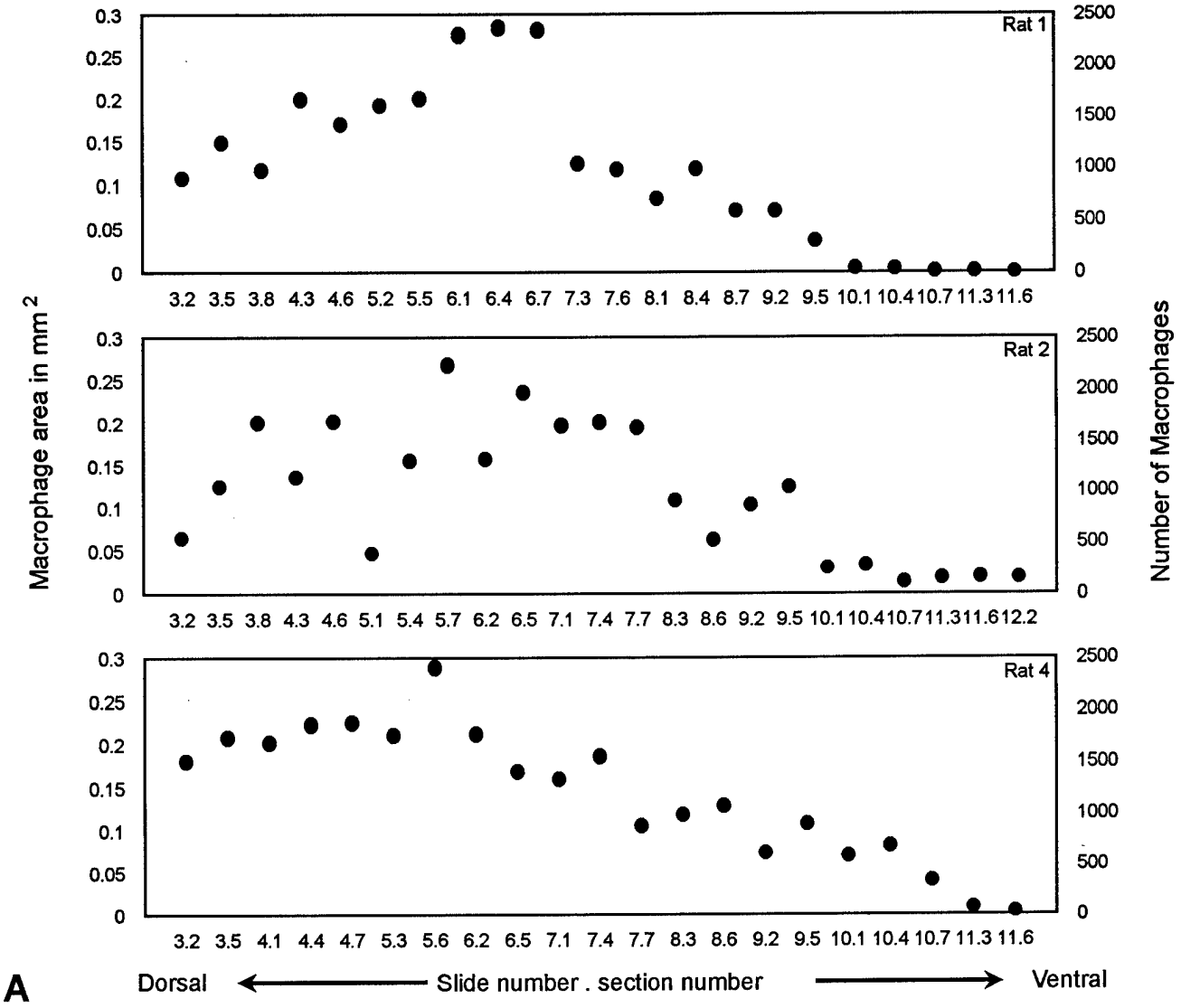
Rat 1
Rat 2
Rat 4
Macrophage area in mm 2
Number of Macrophages
0.3
0.25
0.2
0.15
0.1
0.05
0
2500
2000
1500
1000
500
0
3.2 3.5 3.8 4.3 4.6 5.2 5.5 6.1 6.4 6.7 7.3 7.6 8.1 8.4 8.7 9.2 9.5 10.1 10.4 10.7 11.3 11.6
3.2 3.5 3.8 4.3 4.6 5.1 5.4 5.7 6.2 6.5 7.1 7.4 7.7 8.3 8.6 9.2 9.5 10.1 10.4 10.7 11.3 11.6 12.2
3.2 3.5 4.1 4.4 4.7 5.3 5.6 6.2 6.5 7.1 7.4 7.7 8.3 8.6 9.2 9.5 10.1 10.4 10.7 11.3 11.6
A
Dorsal
Slide number . section number
Ventral

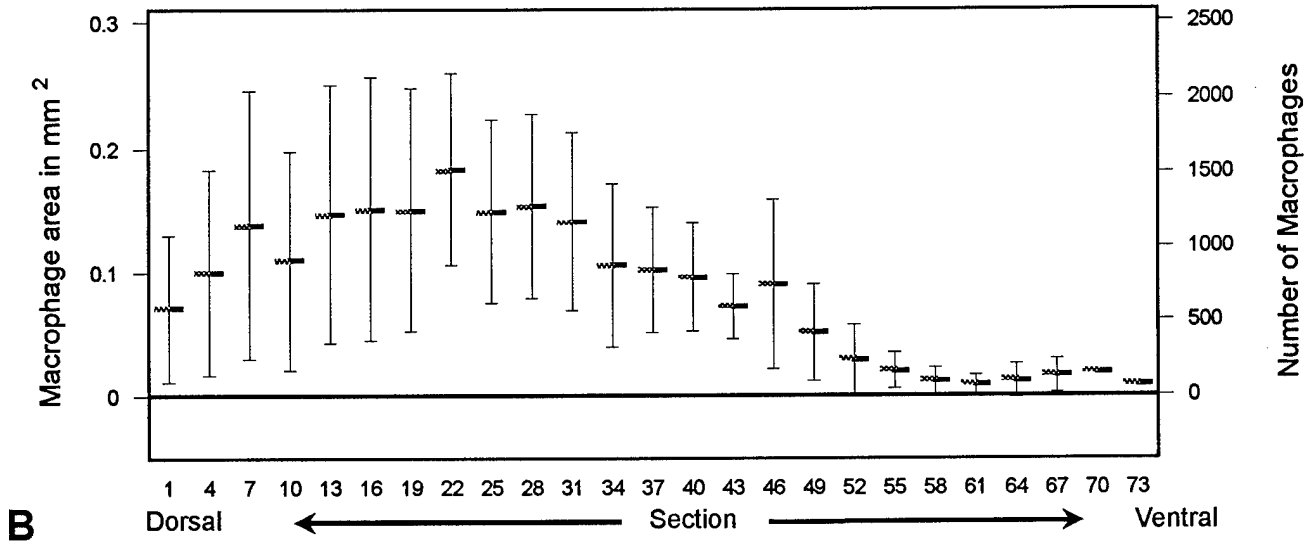
Macrophage area in mm 2
Number of Macrophages
0.3
0.2
0.1
0
2500
2000
1500
1000
500
0
1 4 7 10 13 16 19 22 25 28 31 34 37 40 43 46 49 52 55 58 61 64 67 70 73
B
Dorsal
Section
Ventral

Figure 1

Another commonly observed form of cystic cavitation in all animals was so called "microcavitation". These cavities were not necessarily associated with the focal area of damage. In particular regions of microcavitation were sometimes extensive in white matter tracts undergoing Wallerian degeneration. For example long tracts such as the ascending dorsal columns and lateral white matter tracts were intact on the caudal side of the injury, but degenerate on the rostral side - sometimes for the entire length of the histological segment examined. Phagocytosis of these distal segments produced expanses of cystic white matter where the average diameter of the cysts were curiously about one macrophage cell diameter (15 + 5 μm; n=90; Table 3). It is likely this phagocytosis occurred prior to our sample time of 3 weeks as these cystic regions of white matter did not contain the dense accumulation of macrophages that were observed at the focal region of spinal cord originally compressed. In three of the eight spinal cords containing degenerate white matter tracts, these regions were nearly free of labeled cells. Furthermore, the lateral boundaries of damaged, cystic, spinal cord parenchyma was also relatively free of phagocytes, suggesting the temporal spread of the injury was centripetal.

Cystic regions within the injury zone

Computer assisted two dimensional counting allowed an accurate approximation of the total unit area of cysts at the lesion site, since large cavities within the region of damage could be color transformed and their unit area measured in pixels in much the same manner as performed with single macrophage cells (refer to annual report covering Year 1, 8/94-8/95). The overall size of large cysts found rostrally was not significantly different than in caudal regions of the zone of spinal cord injury. The total unit area of these cysts ranged from about 0.025 - 0.1 mm^2 within the vertebral segment of lesioned cord. Fig. 2 shows three representative examples of such measured cysts (A) and a summary figure (Fig. 2B) for all eight spinal cords studied. Note that in contrast to the character of macrophage accumulations, the regions of spinal cord containing the greatest density of cysts does not correlate with the region of greatest experimental compression. In other words, peaks in cystic cavitation occur over the entire dorsal/ventral extent of the injury zone, and are not confined to the dorsal hemisphere.

Further Methodological Advancements in Computer Assisted Morphometry: Three Dimensional Shape and Volume Reconstruction

In our last report we detailed our new computer assisted quantitative approaches in evaluating the role of macrophage infestation and astrocyte hyperplasia of acute CNS injuries, and the way steady DC voltage gradients may affect these processes leading to a better functional outcome. To more properly visualize these lesions and their cellular components we have developed new three dimensional reconstruction techniques for soft tissue

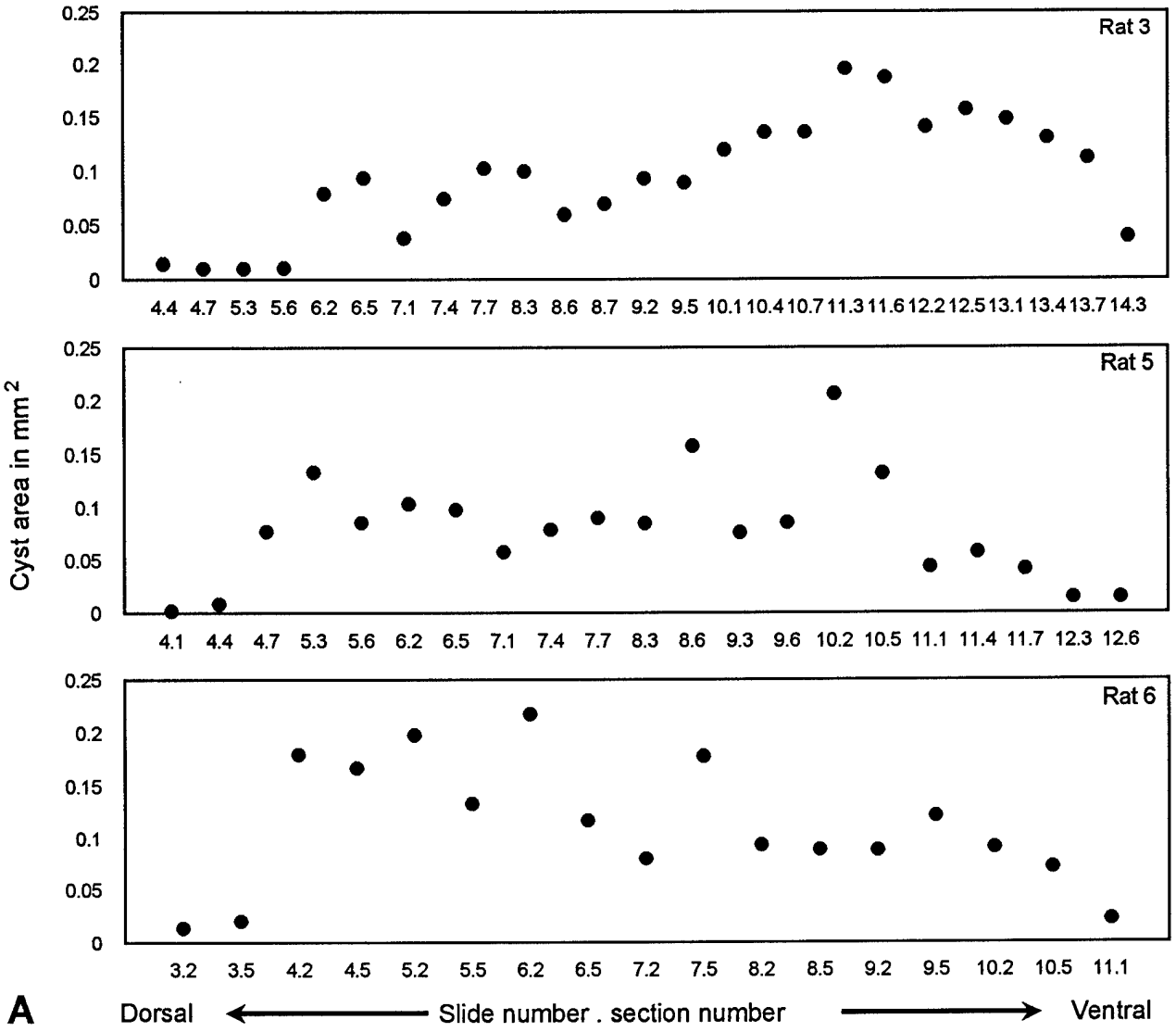
Rat 3
0.25
0.2
0.15
0.1
0.05
0
4.4 4.7 5.3 5.6 6.2 6.5 7.1 7.4 7.7 8.3 8.6 8.7 9.2 9.5 10.1 10.4 10.7 11.3 11.6 12.2 12.5 13.1 13.4 13.7 14.3
Rat 5
Cyst area in mm2
4.1 4.4 4.7 5.3 5.6 6.2 6.5 7.1 7.4 7.7 8.3 8.6 9.3 9.6 10.2 10.5 11.1 11.4 11.7 12.3 12.6
Rat 6
3.2 3.5 4.2 4.5 5.2 5.5 6.2 6.5 7.2 7.5 8.2 8.5 9.2 9.5 10.2 10.5 11.1
A
Dorsal
Slide number . section number
Ventral

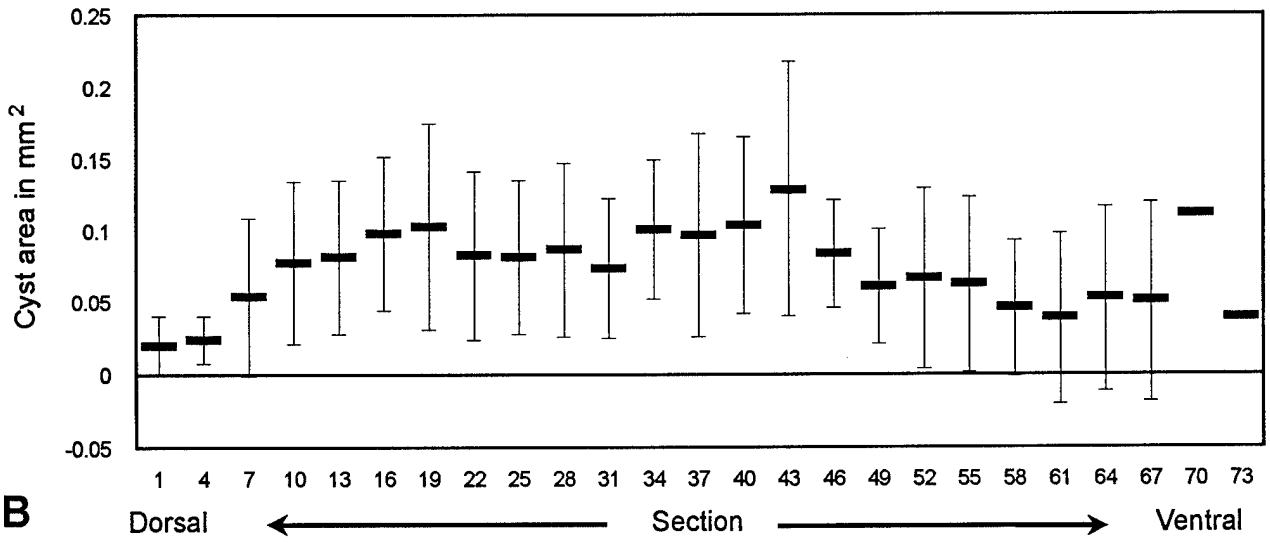
Cyst area in mm2
0.25
0.2
0.15
0.1
0.05
0
-0.05
1 4 7 10 13 16 19 22 25 28 31 34 37 40 43 46 49 52 55 58 61 64 67 70 73
B
Dorsal
Section
Ventral

Figure 2

injury (in collaboration with Professor C. Bajaj, Department of Computer Science, Purdue University). During this last contract year, we have applied these to our studies of spinal injury in progress.

The most recent attempt at three dimensional reconstruction of a laboratory induced spinal cord injury in the rat was attempted by Bresnahan[2] These investigators used histopathological tissue sections of impact/contusion injuries to derive data sets. Individual cross sections of the spinal cord through the region of the lesion were hand traced, emphasizing the boundaries of the spinal cord and the lesioned region contained within it. The individual histological sections used to produce the tracings were not serial. A qualitative evaluation of the derived 3D model was attempted, and a generalized geometric formula (describing a simple biconal geometry) was applied to the model to generate estimates of the relevant surface areas and volumes of the spinal cords and imbedded structures (such as the lesion). Such indirect methods and the secondary mathematical modeling derived from such a 3D visualization, yield substantive oversimplifications. In part because of the difficulty of establishing, and rendering, boundaries and surfaces in soft tissue and injuries to soft tissue, little progress has been made in spinal cord injury since the seminal effort just described. Furthermore, while a literature is emerging on three dimensional visualization of MRI derived clinical head and spinal cord injury data[3] using commercial software tools (see below) - we know of no similar analysis of laboratory produced (standardized) injury models.

Model reconstruction from voxel image data has been an active research area for many years. The principal techniques are contour interpolation and hierarchical volume subdivision. Most algorithms construct polygonal boundary models. Relatively little has been achieved in approximating soft tissue and its pathology with smooth, spatial models bounded by curved surface patches.

Smooth contour interpolation constructs C^1 piecewise smooth approximation in the data slices. Pratt[4] computes conic splines and Nielson and Foley[5] compute parametric B-splines. Bajaj and Xu[6,7] use cubic algebraic splines (A-splines) to achieve higher accuracy fits together with high piecewise continuity. The stack of contours are then interpolated or least-squares approximated with tensor splines, smooth triangular spline patches, or smooth surfaces.

The research described above demonstrates the feasibility of shape reconstruction from volumetric data, but does not provide algorithms that meet the computational needs, indeed demands, of refined biomedical research. Polygonal models are inappropriate for modeling soft tissue. They require far more elements than do smooth models to achieve a given accuracy. Modern graphics hardware can display the smooth models faster and better than the polygonal models. Incremental modification is difficult because changes in one vertex can effect the entire model. The derivative discontinuities increase model error, degrade dynamical simulation, stress analysis, and shading.

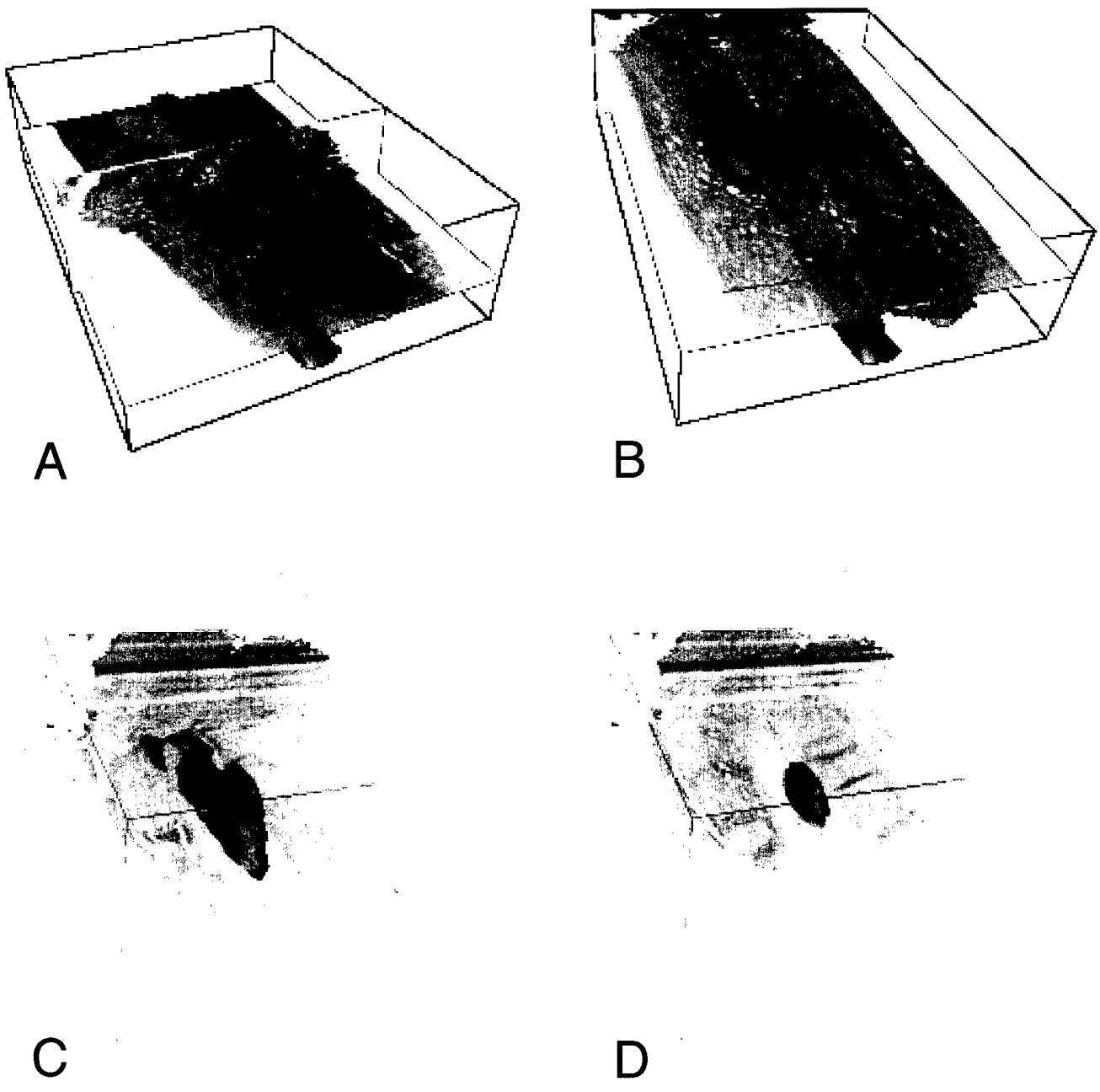

Figure 3 Surface Reconstructions of an Injured Rat Spinal Cord

3-D reconstructions of the zone of injury and the boundary of the spinal cord superimposed within two orthogonal slices of the original histological data set. The lesion boundary was defined by ED-1 labeled phagocytes. A and B represent two views of the same spinal cord (rat 5), with different planes of view represented. C and D are from another data set (rat 32). The ventral surface of the cords are facing upwards. Note the registration of the surface model within the histological section.

Smooth models solve these problems, but complicate reconstruction. The best current algorithms can fail on seemingly straightforward problems.
Three dimensional reconstructions of our digitized images are shown in Figures 3 and 4. Such reconstructions are now being evaluated quantitatively through the development of algorithms to provide volume and surface area of the sub components of the images (for example volume of the cystic regions or surface area of the injury zone). **Table 3** shows such quantitative date derived from the reconstructed data sets shown in Figure 3 and 4 (Rat 5 and 32). This venture has produced novel tools for evaluating and comparing experimental treatments such as the application of exogenous voltages, however at this writing, we have not yet broken the code on all animals in which such computer assisted morphometry and reconstruction has been applied.

Table 3 3D Quantitative Evaluation from Surface Topology

	Surface area (mm^2)	Volume (mm^3)
Rat 5		
cord	46.3	9.2
lesion	20.2	1.5
cysts	9.24	0.1
island	0.50	0.0
lesion+island	20.7	1.5
cord+lesion	N/A	7.5
lesion+cysts	N/A	1.6
Rat 32		
cord	62.5	14.2
lesion	12.9	0.8
cysts	6.92	0.0
cord+lesion	N/A	13.4
lesion+cysts	N/A	0.8

Applied Voltages Decrease the Density of macrophages at the lesion, and reduce cavitation of Spinal Cord Parenchyma

Table 4 reports a summary of data derived from rats in which an applied voltage gradient of approximately 500 μV mm was imposed using indwelling, current regulated stimulators of a previously reported design[8]. These impose a steady voltage gradient for the entire period of study until animal sacrifice at three weeks post injury. The electrodes were affixed to paravertebral musculature and did not touch the spinal cord which was compressed[1] at the mid thoracic level. Control rats (C) were implanted with sham stimulators, indistinguishable from the active units, and all data derived from blinded evaluation. This preliminary evaluation is of 2D morphometry (we have not yet completed 3D quantitative morphometry, see above), and yet requires our volume data to

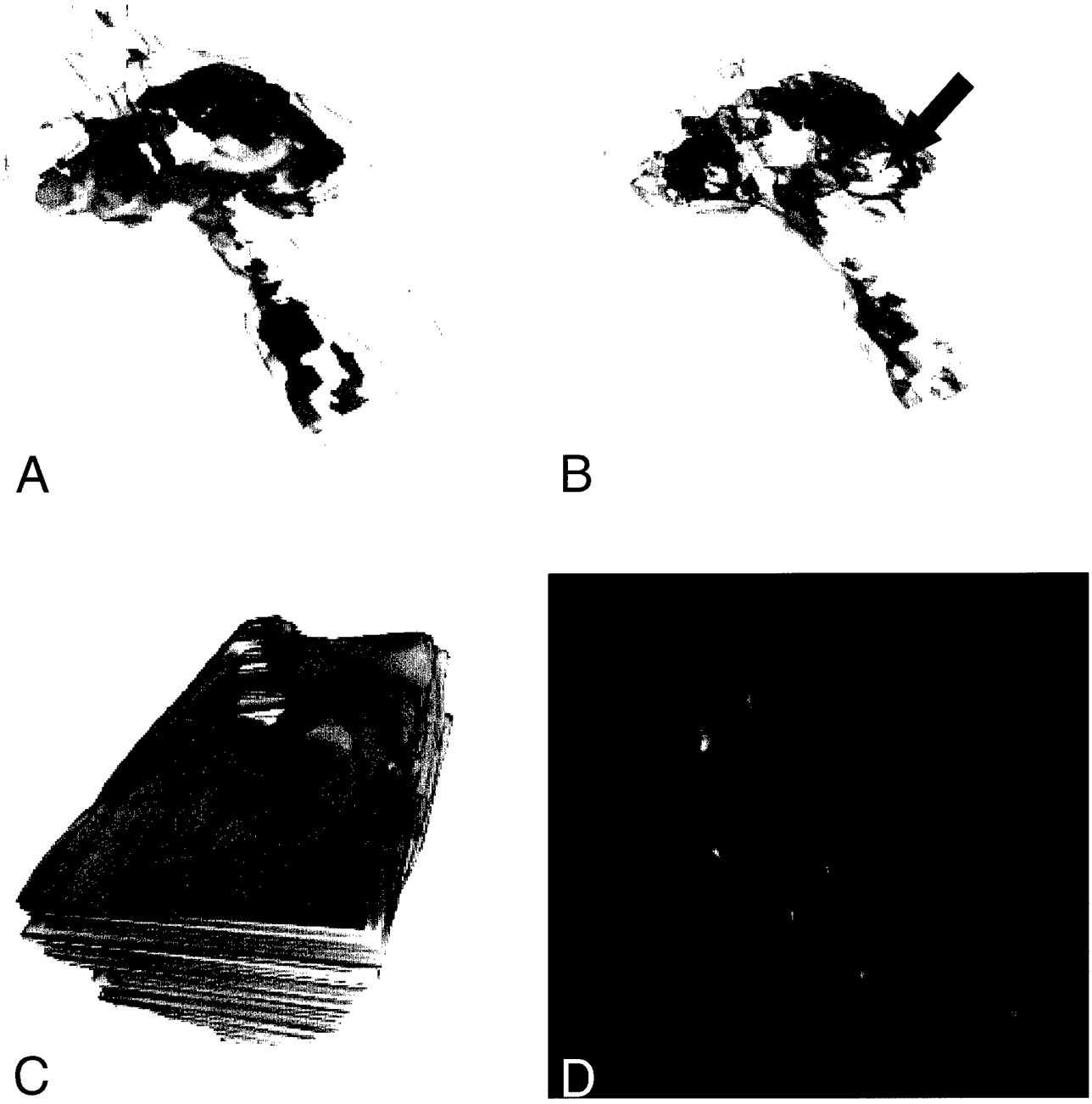

Figure 4

Surface visualizations of the zone of spinal cord injury three weeks post-surgery. Note the reconstruction of cysts (red) within the lesion. In B, a similar view, additionally containing a wire frame reconstruction of a floating "island" of phagocytes (arrow) contained within a large cyst. C shows a wire frame surface model of another spinal lesion (3 weeks following injury) in a rat. The blue surface surrounding the wire frame is the outside perimeter of that segment of spinal cord containing the lesion. In D, the same lesion as shown in C is visualized and contains three dimensional reconstructions of the cysts (red) embedded within it.

normalize this data for macrophage density and % area of cavitation. However, it is already clear that field - treated animals show a consistent lower macrophage count (on the order of about 5%) than controls, as well as a reduction in the percent cavitation of spinal cord parenchyma. While our quantitative evaluation and statistical comparisons are not at this time completed, the trends are in the right direction if our hypotheses are correct. Stated again, that by providing guidance cues facilitating activated phagocyte migration away from the site of damage, the deleterious effects of their excessive numbers in CNS injury may be as well lowered. This may lead to an improved outcome. We are guardedly optimistic that the galvanotactic responses of macrophages noted in vitro[9], may also occur in vivo. Moreover, this data also suggests that in addition to neurons, another cellular target of the voltage gradient applied to acute spinal cord injuries may be these professional scavengers.

Table 4

Rat #	C/E[1]	Number of sections sampled	Macrophage count per cord	Macrophage area[2](mm^2) per cord	Sampled area(mm^2) per cord	Percent macrophages per cord	Percent cavitation per cord
m4	E	21	26828	3.3	12.3	26.5	15.6
m13	E	35	28367	3.4	16.9	20.4	20.9
m15	E	24	42448	5.2	10.3	50.0	19.6
m16	E	27	12299	1.5	10.2	14.6	10.1
m18	E	32	25235	3.1	14.8	20.8	18.4
m19	E	21	11511	1.4	13.6	10.3	23.3
m26	E	28	25760	3.1	16.2	19.3	65.5
m33	E	13	4044	0.5	7.1	7.0	13.3
m34	E	24	17808	2.2	10.4	20.8	22.6
Mean		**25**	**21589**	**2.6**	**12.4**	**21.1**	**23.2**
m5	C	22	21656	2.6	10.7	24.6	26.4
m8	C	23	22587	2.7	9.5	29.0	8.5
m9	C	25	7721	0.9	12.2	7.7	19.2
m14	C	21	24955	3.0	9.7	31.3	12.2
m22	C	21	13700	1.7	9.9	16.7	16.6
m24	C	17	12770	1.5	6.7	23.2	28.1
m32	C	23	10864	1.3	8.5	15.4	10.7
m37	C	11	18581	2.3	4.9	45.9	10.8
Mean		**20**	**16604**	**2.0**	**9.0**	**24.2**	**16.6**

[1]E = experimental, C = control
[2]Total unit area of macrophages comprising lesion

Nerve Regeneration through polymeric tubes in the spinal cord facilitated by an Applied Voltage Gradient

Regeneration of spinal axons can be initiated into tube-like fasciculation pathways in many different contexts. These fasciculation pathways can be special polymeric tubes, fascicles of carbon fibers, and peripheral nerve trunks in which the connective tissue scaffolding of the nerve trunk is present (but no longer contains any axons). We have completed studies where we have implanted polymeric tubes (0.020 inches I.D. by 0.037 inches O.D., 6 mm in length), within the dorsal funiculus of the spinal cord to provide such a pathway, and to determine the extent of axonal regeneration into the tube. Furthermore, we have added an experimental application where a weak (50 uV) current is drawn into each end of the implanted tube by means of a small (40 gauge) platinum cathode imbedded within the center of the bore of the tube. The circuit is completed by implantation of the anode in the paravertebral musculature. The voltage source driving the current is implanted in the fat pad at the base of the guinea pigs neck. **Table 5** below provides summary figures for the 32 animals (Controls and Experimental) in which this procedure has been carried out. Briefly, striking robust regeneration into both ends of the tube is seen in 50% of the experimentals, while control animals show evidence of very limited axonal projections into the open bore of the tube (19% of the population). Axonal projections were visualized by rhodamine dextran injection into the dorsal funiculus two vertebral segments on either side of the implanted tube at the end of the 2 month period of treatment. We provided examples of this anatomical technique in the last progress report and will not include examples of the present study at this time since axonal counting, photography, and three dimensional reconstruction of the tubes is not complete at this time. The table is meant to demonstrate our progress, and full details of this experiment will be included in next years report.

Table 5 Axons in the Tube

	Number of Animals	*<5 axons*	*<20*	*<100*	*>100*	*No Axons*
Experimental (tube &current 0.1uA)	6	0	1	1	1	3
Controls (tube only)	16	3	1	0	0	12

III. CONCLUSIONS

1) During this contract year, the development of novel algorithms for three dimensional volume visualization and shape reconstruction of spinal cord injuries has greatly expanded our ability to evaluate the success of experimental treatments. Furthermore the additional capability to precisely quantitate various aspects of the lesion (i.e. the volume and surface area of cystic cavitation, numbers of identified cell types such as macrophages, the overall topology of the lesion etc.) may have general importance to soft tissue injury evaluation in medicine and surgery.

2) Macrophage invasion of the early CNS injury is profound. These cells occupy up to 80% of the acute and subacute lesion, closely associated with the development of spreading cystic cavitation of CNS parenchyma. These new data strongly support the hypothesis of a hyperbolic inflammatory reaction in injured CNS as a major contributor to functional deficits.

3) Applied voltages are known to influence the migration (galvanotaxis and galvanotropism) of fully activated macrophages. Our preliminary results (still under analysis) is that this may as well occur in vivo during the application of exogenous voltage gradients to acute CNS injuries. Bidirectional movement of phagocytes away from the central lesion may reduce the degree of delayed secondary injury to spinal cord parenchyma.

4) Applied voltages can be used in conjunction with polymeric tubes (fasciculation pathways) to promote strong guidance cues for facilitated nerve regeneration.

IV. REFERENCES

1. Blight A.R. (1991) Morphometric analysis of a model of spinal cord injury in guinea pigs, with behavioral evidence of delayed secondary pathology, *Journal of the Neurological Sciences* 103:156-171.

2. Bresnahan, J.C., Beattie, M.S., Stokes, B.T., and Conway, K.M. (1991) Three-dimensional computer-assisted analysis of graded contusion lesions in the spinal cord of the rat. *J. Neurotrauma.* 8:91-101

3. Chakers, W.D., Flickinger, F., Bresnahan, C.J., Beattie, M.S., Weiss, K.L., Miller, C., and Strokes, B. (1987) MR imaging of the acute spinal cord trauma. *Annual Journal of Neurological Research* 8:5-10.

4. Pratt, V. (1985) Techniques for conic splines. *Computer Graphics*, 19(3):151-159.

5. Nielson, G. and T. Foley. (1989) Knot Selection for Parametric Spline Interpolation. In T. Lyche and L. Schumaker, editors, *Mathematical Methods in Computer Aided Geometric Design*, pages 261-271. Academic Press.

6. Bajaj, C. and G. Xu. (1992) *A-Splines: Local Interpolation and Approximation using Continuous Piecewise Real Algebraic Curves.* Computer Science Technical Report, CAPO-92-44, Purdue University.

7. Bajaj, C. and G. Xu. (1994) Data Fitting with Cubic A-Splines. In *Proceedings of Computer Graphics International '94*, pages x-y, Melbourne, Australia.

8. Borgens, R.B., A.R. Blight, D.J. Murphy, and L. Stewart (1986). Transected dorsal column axons within the guinea pig spinal cord regenerate in the presence of an applied electric field. *J. Comp. Neurol.* 250:168-180.

9. Orida and Feldman (1982) Directional Protrusive Pseudopodial Activity and Motility in Macrophages Induced by Extracellular Electric Fields. *Cell Motility* 2:243-255.